



3D thermo-chemical-mechanical analysis of the pultrusion process

Baran, Ismet; Hattel, Jesper Henri; Tutum, Cem C.

Published in:

Proceedings of the Risø International Symposium on Materials Science

Publication date:

2013

Document Version

Publisher's PDF, also known as Version of record

[Link back to DTU Orbit](#)

Citation (APA):

Baran, I., Hattel, J. H., & Tutum, C. C. (2013). 3D thermo-chemical-mechanical analysis of the pultrusion process. *Proceedings of the Risø International Symposium on Materials Science*, 34, 169-176.

General rights

Copyright and moral rights for the publications made accessible in the public portal are retained by the authors and/or other copyright owners and it is a condition of accessing publications that users recognise and abide by the legal requirements associated with these rights.

- Users may download and print one copy of any publication from the public portal for the purpose of private study or research.
- You may not further distribute the material or use it for any profit-making activity or commercial gain
- You may freely distribute the URL identifying the publication in the public portal

If you believe that this document breaches copyright please contact us providing details, and we will remove access to the work immediately and investigate your claim.

3D THERMO-CHEMICAL-MECHANICAL ANALYSIS OF THE PULTRUSION PROCESS

I. Baran*, J.H. Hattel* and Cem C. Tutum**

* Technical University of Denmark, Department of Mechanical
Engineering, Denmark

** Michigan State University, Department of Electrical and Computer
Engineering, East Lansing, MI, USA

ABSTRACT

In the present study, a 3D Eulerian thermo-chemical analysis is sequentially coupled with a 3D Lagrangian quasi static mechanical analysis of the pultrusion process. The temperature and degree of cure profiles at the steady state are first calculated in the thermo-chemical analysis. In the mechanical analysis, the developments of the process induced stresses and distortions during the process are predicted using the already obtained temperature and degree of cure profiles together with the glass transition temperature. The predictions of the transverse transient stresses and distortions are found to be similar as compared to the available data in the literature. Using the proposed 3D mechanical analysis, different mechanical behaviour is obtained for the longitudinal stress development as distinct from the stress development in the transverse directions. Even though the matrix material is in a liquid state before entering the die (the degree of cure is zero), it is found that there exists longitudinal stresses at the mid-section which indicates that the already pulled material has an effect on the longitudinal stress evolution even before entering the die.

1. INTRODUCTION

Pultrusion is one of the cost efficient composite manufacturing processes in which constant cross sectional continuous fiber reinforced plastic (FRP) profiles are produced. Recently, pultruded structures are foreseen to have potential for the replacement of conventional materials used in the construction industry. More specifically, the application of pultruded composite rods is significantly increasing for reinforcements of concrete elements in the construction industry. This has lead to an increased need for a detailed understanding of the mechanical behavior as well as the failure mechanism of the profile. A schematic view of the pultrusion process is depicted in Fig. 1.

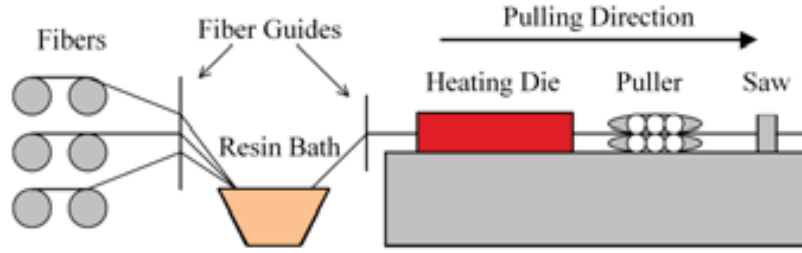


Fig. 1. Schematic view of the pultrusion domain for the composite rod. Fibers/mats and resin matrix are pulled together in the pultrusion direction by pullers through the heated die and then the cured composite is cut by a saw system.

Process induced residual stresses and shape distortions may be important for pultruded products such as reinforcement profiles in the construction industry, stiffeners for wind turbine blades, window frames and fencing panels. Hence, the process induced variations should be controlled or avoided during process which may arise due to the certain mechanisms [Svanberg and Holmberg (2001), Wisnom, Gigliotti, Ersoy, Campbell and Potter (2006), Bogetti and Gillespie Jr (1992), Johnston (1997)]: (i) the mismatch in the coefficient of thermal expansion (CTE) of the matrix material and the reinforcement material (fibers, mats etc.), (ii) the chemical shrinkage of the matrix material, (iii) the tool-part interaction and (iv) the temperature and the degree of cure gradients through the composite thickness due to non-uniform curing. In order to have a better understanding of the pultrusion process, several numerical models have been developed in the literature [Baran, Tutum, and Hattel (2012a), Baran, Tutum, and Hattel (2012b), Baran, Tutum, and Hattel (2012c), Baran, Tutum, and Hattel (2013a), Baran, Tutum, and Hattel (2013b), Baran, Tutum, Nielsen and Hattel (2013c), Chachad, Roux, Vaughan, and Arafat (1995), Carlone, Palazzo and Pasquino (2006), Carlone and Palazzo (2007), Carlone and Palazzo (2008), Joshi, Lam and Win Tun (2003), Liu, Crouch, and Lam (2000), Tutum, Baran and Hattel (2013)].

In the present work, the 3D process induced transverse stresses and distortions are predicted using the finite element method (FEM) for the pultrusion of a glass/epoxy square beam. The temperature and the cure degree distributions are calculated in the 3D thermo-chemical simulation. By using these distributions, the 3D transient stresses and distortions are calculated by means of the cure hardening instantaneous linear elastic (CHILE) approach [Johnston (1997)], which is a valid pseudo-viscoelastic approximation of the linear viscoelasticity.

2. THERMO-CHEMICAL MODEL

2.1 Numerical Implementation. In the thermo-chemical model, the energy equations for the square composite beam and the die block domains given in Eq. 1 and Eq. 2, respectively, are solved in order to calculate the temperature field.

$$\rho_c C p_c \left(\frac{\partial T}{\partial t} + u \frac{\partial T}{\partial x_3} \right) = k_{x_1,c} \frac{\partial^2 T}{\partial x_1^2} + k_{x_2,c} \frac{\partial^2 T}{\partial x_2^2} + k_{x_3,c} \frac{\partial^2 T}{\partial x_3^2} + q \quad (1)$$

$$\rho_d C p_d \frac{\partial T}{\partial t} = k_{x_1,d} \frac{\partial^2 T}{\partial x_1^2} + k_{x_2,d} \frac{\partial^2 T}{\partial x_2^2} + k_{x_3,d} \frac{\partial^2 T}{\partial x_3^2} \quad (2)$$

where T is the temperature, t is the time, u is the pulling speed, ρ is the density, Cp is the specific heat and k_{x1} , k_{x2} and k_{x3} are the thermal conductivities along the x_1 , x_2 and x_3 directions,

respectively. The subscriptions c and d correspond to composite and die, respectively. Lumped material properties are used and assumed to be constant throughout the process. The internal heat generation (q) [W/m^3] due to the exothermic reaction of the epoxy resin can be expressed as [Chachad et al. (1995), Baran et al. (2013c)]:

$$q = (1 - V_f) \rho_r H_{tr} [R_r(\alpha)]_e \quad (3)$$

where V_f is the fiber volume fraction and H_{tr} is the total heat of reaction, ρ_r is the density of epoxy resin, α is the degree of cure and $[R_r(\alpha)]_e$ is the effective cure rate, i.e. $d\alpha/dt$, expressed as [Chachad et al. (1995), Baran et al. (2013c)]

$$[R_r(\alpha)]_e = K_o \exp\left(-\frac{E}{RT}\right) (1 - \alpha)^n \cdot f(\alpha, T) \quad (4)$$

where K_o is the pre-exponential constant, E is the activation energy, R is the universal gas constant and n is the order of the reaction (kinetic exponent). K_o , E , H_{tr} and n can be obtained by a curve fitting procedure applied to the experimental data evaluated using differential scanning calorimetry DSC [Chachad et al. (1995)]. $f(\alpha, T)$ is the diffusion factor which accounts for the glass transition effect defined as [Johnston (1997)]:

$$f(\alpha, T) = \frac{1}{1 + \exp[C(\alpha - (\alpha_{c0} + \alpha_{CT}T))]} \quad (5)$$

where C is a diffusion constant, α_{c0} is the critical degree of cure at $T = 0$ K and α_{CT} is a constant for the increase in critical α with T [Johnston (1997)]. The relation of the effective resin kinetics equation can be expressed as [Baran et al. (2013c)]

$$\frac{\partial \alpha}{\partial t} = [R_r(\alpha)]_e - u \frac{\partial \alpha}{\partial x_3} \quad (6)$$

where it is the expression in Eq. 6 which is used in the numerical model.

For the 3D thermo-chemical simulation of the pultrusion process, user defined sub-routines in a commercial finite element software ABAQUS (version 6.11, 2011) are used in order to obtain the temperature and degree of cure fields.

2.2 Model description. The 3D thermo-chemical simulation of the pultrusion of a UD glass/epoxy based square beam is carried out. Only a quarter of the pultrusion domain is modelled due to symmetry. The details of the model geometry and the dimensions are given in Fig. 2. Material properties are listed in Table 1. The resin kinetic parameters are [Chachad et al. (1995), Baran et al. (2013c)]: $H_{tr} = 324$ (kJ/kg), $K_o = 192000$ (1/s), $E = 60$ (kJ/mol), $n = 1.69$, $C = 30$, $\alpha_{c0} = -1.5$ and $\alpha_{CT} = 0.0055$ (1/K). At the symmetry surfaces adiabatic boundaries are defined in which no heat flow is allowed across the boundaries. The remaining exterior surfaces of the die are exposed to ambient temperature (27 °C) with a convective heat transfer coefficient of 10 W/(m² K) except for the surfaces located at the heating regions. Similarly, at the post die region, convective boundaries are defined for the exterior surfaces of the pultruded profile. The length of the post die region (L_{conv} in Fig. 2) is determined to be approximately 13.7 m [Baran et al. (2013c)] which results in a total length of approximately 14.6 m ($L_{die} + L_{conv}$, Fig. 2) for the composite part.

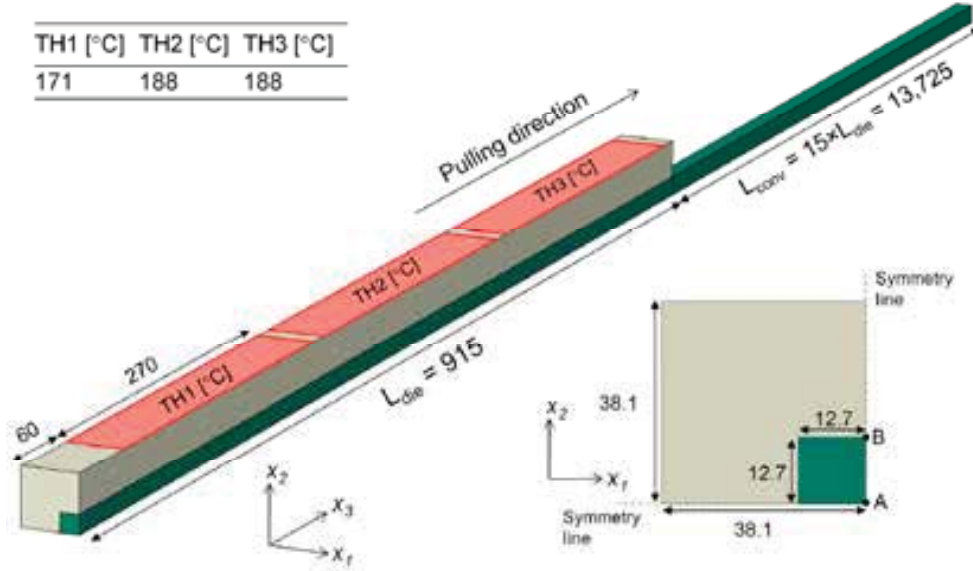


Fig. 2. Schematic view of the pultrusion domain for the square beam. All dimensions are in mm.

Table 1. Material Properties [Chachad et al. (1995)].

Material	ρ (kg/m ³)	C_p (J/kg K)	k_{x_3} (W/m K)	k_{x_1}, k_{x_2} (W/m K)
Composite ($V_f = 63.9\%$)	2090.7	797.27	0.9053	0.5592
Die (steel)	7833	460	40	40

3. THERMO-CHEMICAL-MECHANICAL MODEL

3.1 Numerical implementation. The effective mechanical properties of the composite are calculated by using the self consistent field micromechanics (SCFM) approach which is a well known technique in the literature [Bogetti and Gillespie Jr (1992)]. The instantaneous resin elastic modulus development during the process is calculated using the CHILE approach. The glass transition temperature (T_g) is calculated using Di Benedetto equation [Johnston (1997)]. An incremental linear elastic approach is implemented utilizing user-subroutines in ABAQUS for the calculation of the residual stresses and distortions as used in. In the present study, the total volumetric shrinkage of the epoxy resin is assumed to be 6% [Baran et al. (2013c)].

3.2 Model description. The developments of the 3D process induced stresses and distortions are predicted using a 3D thermo-chemical-mechanical model. In this model, the 3D composite part defined in Section 2 is assumed to move along the pulling direction of the process while tracking the corresponding temperature and degree of cure profiles already calculated in the 3D thermo-chemical simulation. In other words, a 3D Eulerian thermo-chemical model is coupled with a 3D quasi-static Lagrangian mechanical model. The die surfaces are not included in the proposed 3D mechanical model. A mechanical symmetry boundary condition (BC) is applied at the symmetry surfaces (see Fig. 2) in the x_1 and x_2 -directions. There is no applied mechanical BC at the ends of the composite part in the x_3 -direction, i.e. a free-free BC is applied at the end surfaces in the x_3 -direction. The corresponding stresses and distortions are calculated based on the temperature and the cure distributions together with the corresponding glass transition temperature (T_g) of the composite part by using the 3D quadratic elements in ABAQUS.

4. RESULTS AND DISCUSSIONS

In order to reflect the 3D thermo-chemical-mechanical behavior of the process more precisely and correctly, the mid-section of the composite part is considered since the pultrusion is a continuous process, i.e. there is always material inside the heating die during the process. The details of the mid-section are shown in Fig. 3 in which a schematic view of the movement of the part in the pulling direction is depicted. It should be noted that the tracking of the mid-section starts at $x_3 \approx -7.3$ m and ends at $x_3 \approx 7.3$ m. The pulling speed is set to 20 cm/minute.

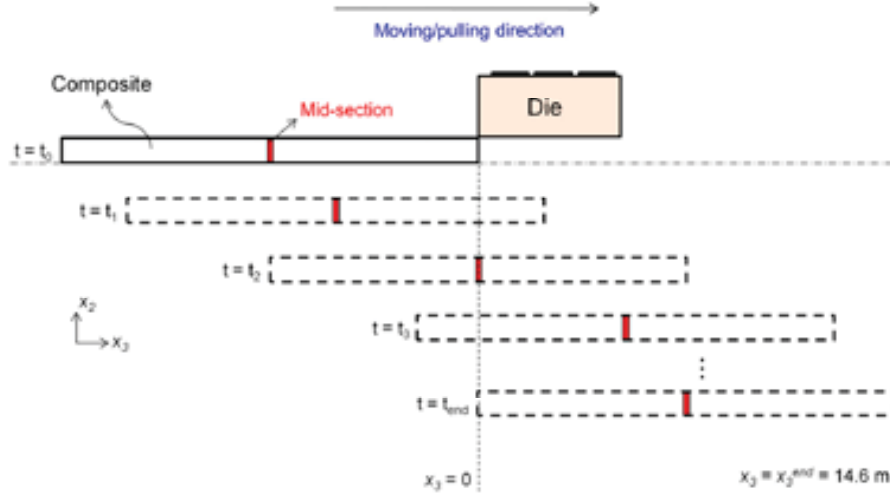


Fig. 3. Schematic view of the movement of the part in the pulling direction and the positioning of the mid-section. The sizes of the die and the part are not scaled.

The transient temperature and degree of cure distributions at the mid-section are shown in Fig. 4 for the inner region (point A) and the outer region (point B). It is seen that until the mid-section enters the heating die, the temperature remains constant as the resin bath temperature of 30°C and the degree of cure remains uncured, i.e. $\alpha = 0$. The non-uniform temperature and degree of cure profiles are obtained especially inside the die, such that the point B cures earlier than the point A since it is closer to the die having heaters on top of it. This shows that the internal heat generation of the matrix material plays a more important role for the inner region (point A). The maximum temperature and degree of cure value obtained inside the composite are approximately 217°C and 0.97, respectively (for point A).

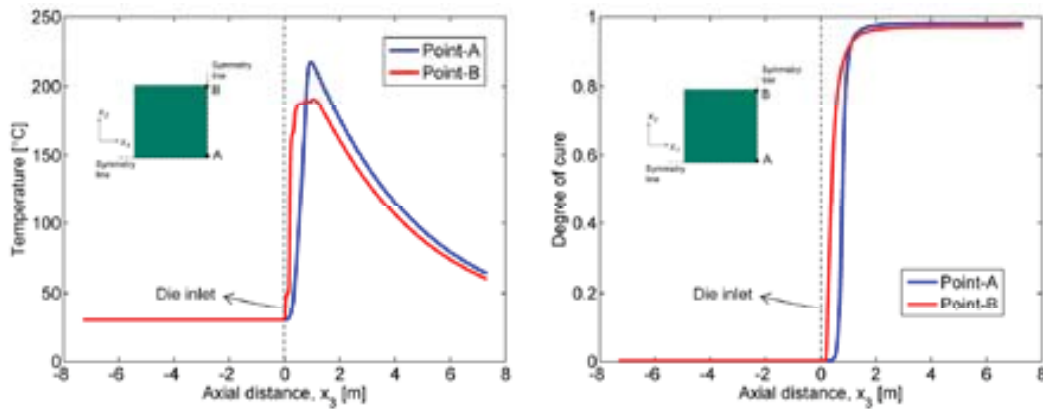


Fig. 4. The temperature (*left*) and degree of cure (*right*) distributions at the mid-section for point A and point B.

The non-uniform temperature and degree of cure distributions promote the process induced residual stresses and distortions [Bogetti and Gillespie Jr (1992)]. The evolutions of the transient stresses at the mid-section (Fig. 3) are given in Fig. 5 for point A and point B. In Fig. 5, S_{11} , S_{22} and S_{33} are the normal stresses in the x_1 -direction (horizontal, transverse), the x_2 -direction (vertical, transverse) and the x_3 -direction (longitudinal), respectively. It is seen that until the mid-section enters the die, there are almost no transverse stresses, i.e. S_{11} and S_{22} (Fig. 5a,b). This shows that the already pulled material (e.g. the front end of the product) has no effect on the stress development at the mid-section. Inside the the die, the stress levels are relatively small because the matrix material has not enough stiffness to build up the stresses. The outer regions closest to the die cure first which make them a little constrained by the inner region during shrinkage. Due to this, a residual compression is found in these regions [Baran et al. (2013c)].

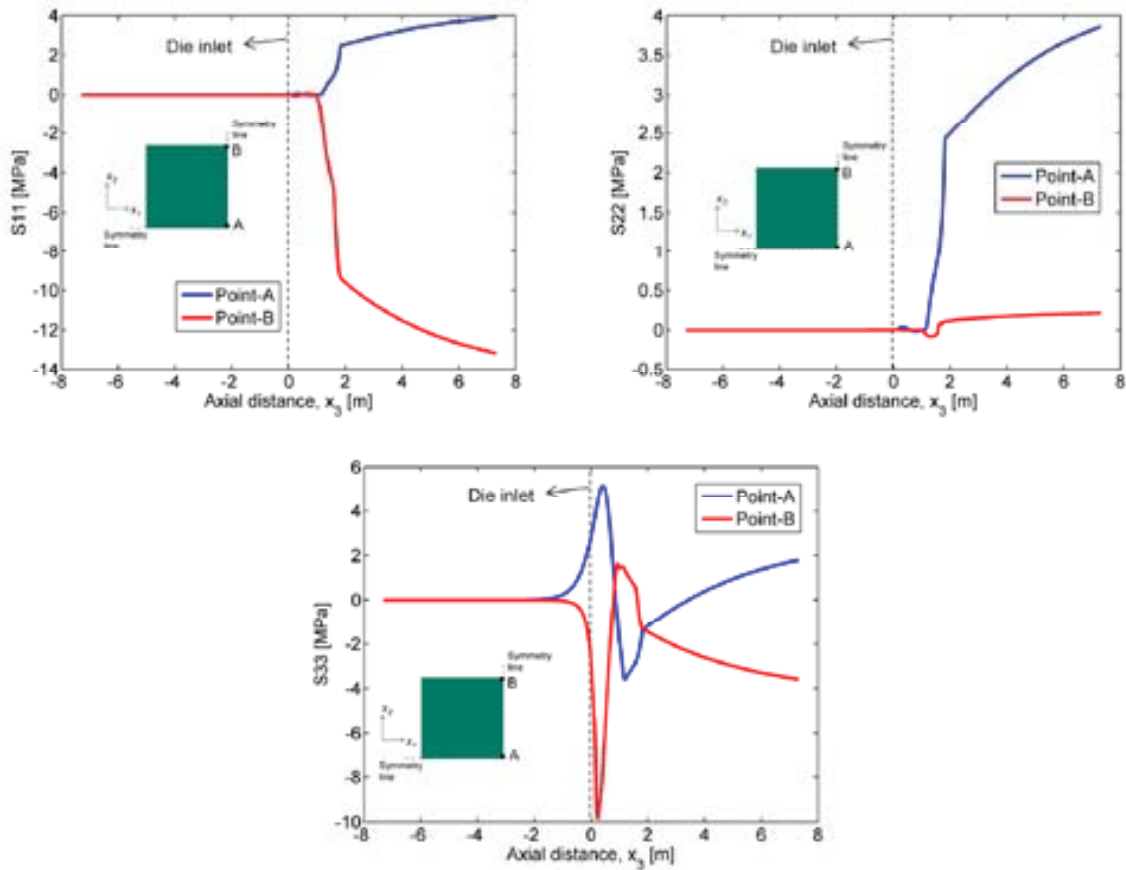


Fig. 5. The transverse transient stress S_{11} (a), S_{22} (b) and the longitudinal stress S_{33} (c) evolutions at the mid-section for point A and point B.

Regarding the longitudinal stress development (S_{33}) in the pulling or fiber direction, different mechanical behaviour is obtained as distinct from the stress development in the transverse directions (S_{11} and S_{22}). Even though the matrix material is in a liquid state before entering the die (the degree of cure is zero), it is found that there exists longitudinal stresses at the mid-section which can be seen in Fig. 5c. This indicates that the already pulled material has an effect on the longitudinal stress evolution at the mid-section even before entering the die. However, as mentioned before, this 3D effect is not pronounced in the transverse directions. It is important that the 3D effect in the longitudinal direction is only captured by using the full 3D mechanical model. The longitudinal stress levels calculated for S_{33} (Fig. 5) are found to be relatively small as compared to S_{11} and S_{22} because the process induced strains in the longitudinal direction are

smaller than the ones in the transverse directions. The fibers in the pulling directions restrict the process induced strain built-up in the longitudinal direction; hence, this provides lower process induced stresses in the longitudinal direction (S33).

The evolution of the displacement profile at the mid-section for point B in the x_2 -direction (U_2) is shown in Fig. 6. It is seen that the part starts expanding while entering the die owing to the increase in temperature and the exclusion of the die surfaces in the present 3D mechanical model. It should be noted that the initial pressure condition of the part before entering the heating die is not taken into account which may affect the stress and displacement field. It is seen from Fig. 6 that the cure shrinkage takes place after approximately 0.5 m from the die inlet which results in a decrease in the displacement value. After that point, the point B shrinks until the end of the process due to cure together with convective cooling at the post die region.

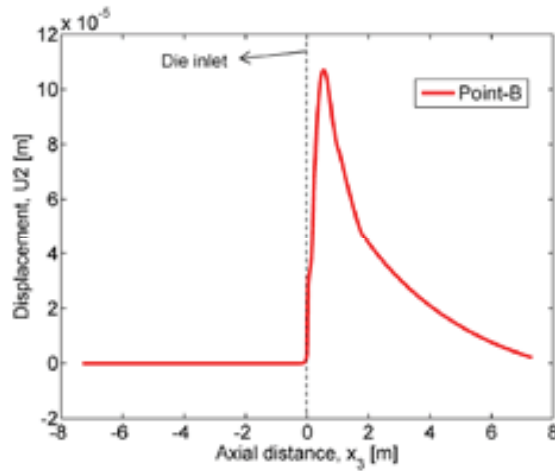


Fig. 6. Displacement of the point B in x_2 -direction (U_2) for the mid-section of the part

5. CONCLUSIONS

In the present work, a 3D Eulerian thermo-chemical model was sequentially coupled with a 3D quasi-static Lagrangian mechanical model for the pultrusion process simulation of a square UD glass/epoxy composite beam. The CHILE approach was implemented for the calculation of the instantaneous resin modulus development. The effective mechanical properties of the composite are calculated using the SCFM method. The transient stress and displacement evolutions are predicted incorporating the temperature and degree of cure profiles. The trend of the transverse stress development was found to be similar as predicted in [Baran et al. (2013c)]. Regarding the longitudinal stress prediction, the effect of the already pulled material on the stress development at the mid-section was investigated in the 3D mechanical model. Longitudinal process induced stresses were found to exist before entering the heating die due to the 3D effect. This is one of the important aspects of the proposed 3D mechanical model which would be very useful for the calculation of the pulling as well as frictional forces during the process. Apart from the transient stresses, the displacement evolution of the product was predicted which would be crucial for pultruded products such as window frames and fencing panels due to their desired high geometrical precision. Hence, the proposed 3D thermo-chemical-mechanical model has the potential for controlling or avoiding the development of process induced shape distortions.

ACKNOWLEDGEMENTS

This work is a part of a DeepWind project which has been granted by the European Commission (EC) under FP7 program platform Future Emerging Technology.

REFERENCES

- Baran, I., Tutum, C.C., and Hattel, J.H. (2012a). Optimization of the thermosetting pultrusion process by using hybrid and mixed integer genetic algorithms. *App. Compos. Mat.* DOI: 10.1007/s10443-012-9278-3.
- Baran, I., Tutum, C.C., and Hattel, J.H. (2012b). Reliability estimation of the pultrusion process using the first-order reliability method (FORM). *App. Compos. Mat.* DOI: 10.1007/s10443-012-9293-4.
- Baran, I., Tutum, C.C., and Hattel, J.H. (2012c). Probabilistic thermo-chemical analysis of a pultruded composite rod. In: *Proceedings of the 15th European Conference on Composite Materials (Venice, Italy, 24-28 June 2012)*.
- Baran, I., Tutum, C.C., and Hattel, J.H. (2013a). The internal stress evaluation of the pultruded blades for a Darrieus wind turbine. *Key Eng. Mat.* 554-557, 2127-2137.
- Baran, I., Tutum, C.C., and Hattel, J.H. (2013b). The effect of thermal contact resistance on the thermosetting pultrusion process. *Compos. Part B: Eng.* 45, 995-1000.
- Baran, I., Tutum, C.C., Nielsen, M.W., and Hattel, J.H. (2013c). Process induced residual stresses and distortions in pultrusion. *Compos. Part B: Eng.* 51, 148-161.
- Bogetti, T. A., and Gillespie Jr, J. W. (1992). Process-induced stress and deformation in thick-section thermoset composite laminates. *J. Compos. Mater.* 26 (5), 626-660.
- Chachad, Y.R., Roux, J.A., Vaughan, J.G., and Arafat, E. (1995). Three-dimensional characterization of pultruded fiberglass-epoxy composite materials. *J. Reinf. Plast. Comp.* 14, 495-512.
- Carlone, P., Palazzo, G.S., and Pasquino, R. (2006). Pultrusion manufacturing process development by computational modelling and methods. *Math. Comput. Model.* 44, 701-709.
- Carlone, P., and Palazzo, G.S. (2007). Pultrusion manufacturing process development: Cure optimization by hybrid computational methods. *Comput. Math. Appl.* 53, 1464-1471.
- Carlone, P., and Palazzo, G.S. (2008). Viscous pull force evaluation in the pultrusion process by a finite element thermo-chemical rheological model. *Int. J. Mater. Form.* 1, 831-834.
- Johnston, A. (1997). *An Integrated Model of the Development of Process-Induced Deformation in Autoclave Processing of Composites Structures*. (Ph.D. thesis, The University of British Columbia, Vancouver).
- Joshi, S.C., Lam, Y.C., and Win Tun, U. (2003). Improved cure optimization in pultrusion with pre-heating and die-cooler temperature. *Compos. Part A: Appl. S.* 34, 1151-1159.
- Liu, X.L., Crouch, I.G., and Lam, Y.C. (2000). Simulation of heat transfer and cure in pultrusion with a general-purpose finite element package. *Compos. Sci. Technol.* 60, 857-864.
- Svanberg, J.M., and Holmberg, J.A. (2001). An experimental investigation on mechanisms for manufacturing induced shape distortions in homogeneous and balanced laminates. *Compos. Part A: Appl. S.* 32, 827-838.
- Tutum, C.C., Baran, I., and Hattel, J.H. (2013). Utilizing multiple objectives for the optimization of the pultrusion process. *Key Eng. Mat.* 554-557, 2165-2174.
- Wisnom, M.R., Gigliotti, M., Ersoy, N., Campbell, M., and Potter, K.D. (2006). Mechanisms generating residual stresses and distortion during manufacture of polymer-matrix composite structures. *Compos. Part A: Appl. S.* 37, 522-529.